A structure-dependent change of magnetism in the magnetic oxide $La_{0.85}Sr_{0.15}MnO_z$

1997 J. Phys.: Condens. Matter 9 4281

(http://iopscience.iop.org/0953-8984/9/20/023)

J. Phys.: Condens. Matter **9** (1997) 4281–4288. Printed in the UK PII: S0953-8984(97)80799-0

A structure-dependent change of magnetism in the magnetic oxide $La_{0.85}Sr_{0.15}MnO_z$

Ning Zhang†‡, Weiping Ding†, Wei Zhong†, Wei Yang† and Youwei Du†

† National Laboratory of Solid State Microstructures, Nanjing University, Nanjing 210093, People's Republic of China

‡ Key Laboratory of JiangSu Province for Optic and Electric Techniques, Nanjing Normal University, Nanjing 210024, People's Republic of China

Received 9 January 1997

Abstract. The grain size dependences of magnetic properties in the granular perovskite $La_{0.85}Sr_{0.15}MnO_3$ have been investigated. A structural phase transition from cubic perovskite to orthorhombic form and lattice parameter enlargements with grain growth have been observed. Simultaneously, a series of magnetic changes, including magnetization and Curie temperature, has been obtained with the change of grain size. These phenomena suggest a structure-coupled change of magnetism in the hole-doped manganese perovskites.

1. Introduction

The close interplay between magnetism and transport properties, in particular the colossal magnetoresistance (CMR), in the perovskite family La–R–Mn–O (R = Sr, Ca, Pb, Ba) has lately absorbed much attention [1–3]. As a function of temperature, doping and structure distortion, this system displays various magnetic transitions, some of which are associated with sharp changes of electric properties. The magnetic transition induced by an external field can lead to a sharp drop of resistivity. This is CMR.

The CMR phenomenon was traditionally attributed to the double-exchange interactions between pairs of Mn^{3+} and Mn^{4+} ions in these manganese oxides. However, an increasing number of experimental data demonstrated that double exchange is incompatible with many aspects, and especially contradicts the lattice distortions coinciding with the emergence of CMR. Although the exact mechanism of CMR remains plausible, it is now believed that the CMR phenomenon, which suggests a close relation between magnetism and conductive properties in this perovskite, relates not only to double exchange but also to structural distortions.

Structure and magnetism can influence on each other in these manganese perovskites as indicated in many papers. An external field can induce structural distortion(s), phase transition [4], or striction [5] in the compound, whereas structural distortion(s) triggered by heating [6], pressing [7], substituting the A-site ion [8], varying oxygen content [9], or changing concentration [10] can also change magnetism, including magnetization M and Curie temperature T_C, thereby changing resistivity, maybe through double exchange. It was found that a change of Mn–O bond length or Mn–O–Mn bond angle or structural variation can all greatly influence the magnetic properties in these perovskites [8, 9, 11]. Nevertheless, the coupling between structure and magnetism is not yet, a well understood problem, although many works have been done on this subject [12–14].

0953-8984/97/204281+08$19.50

In this paper, we first present a study of structure-dependent magnetism though studying grain-size-dependent magnetic properties in the granular perovskite $La_{0.85}Sr_{0.15}MnO_3$ system. A result different from that in $La_{0.67}Ca_{0.33}MnO_3$ [15] has been observed. We will first show lattice distortions with changing crystal grain size in such a CMR oxide, and demonstrate that the distortion could originate in surface stress of small grain by introducing a *liquid drop* model. Through measuring oxygen content, we will show that not oxygen content difference but lattice distortion is mainly responsible for the change of magnetism in the present system. Moreover, we will connect the grain-size-dependent change of magnetism with the grain size dependences of lattice distortions.

2. Theory of surface stress-dependent lattice distortions

A surface, especially the surface of a small grain, often has a lattice structure different from that in the bulk or within the grain [16, 17]. This could induce stresses simultaneously in the surface within the grain, that is very similar to that observed in a thin film deposited on a substrate with a non-matching lattice. The surface stress of a grain could cause a quasi-hydrostastic pressure in the grain, noting that grains are not spherical in shape, as the surface stresses of a liquid drop acts inside the drop. It is well known that the surface stress-induced extra pressure in a liquid drop can be expressed

$$P = \sigma/D \tag{1}$$

where σ is the surface tension coefficient and D is the diameter of a drop. For an arbitrary solid grain, formula (1) appears too rough. Nevertheless, for a grain like ours, which was grown from liquid phase and annealed adequately, formula (1) may be reasonable. Assuming that is true, σ should be given by [18]

$$\sigma = E_s/A = E_s/\pi D^2 \tag{2}$$

where A is the surface area, E_s is the surface energy, which is relative not only to the bond energy of atoms in the surface but also to the lattice structure of the surface, which depends on the process of grain formation. Combining (1) and (2) yields

$$P = E_s/\pi D^3. \tag{3}$$

Formula (3) may be called the *liquid drop* model. According to this, a smaller grain will be acted on by a larger pressure, and the pressure in the grain will rapidly increase with decreasing grain size. Therefore the lattice structure of smaller grains could be more compressed under the pressure induced by surface stress. On the other hand, for an ionic crystal, such as La–Sr–Mn–O, the repulsive potential between two neighbouring ions should follow the Madelung potential, which can be simply written as [19]

$$\psi(r) = B\exp(-r/\rho) \tag{4}$$

where B and ρ are empirical constants and r is the interatom distance. Thus, the force between two neighbouring ions would be $F = -\partial\varphi/\partial r$, while r should be fitted with $P = F$ in the grain. In view of this and (3) and (4), we obtain

$$r = Q_1 + Q_2\ln(D) \tag{5}$$

where Q_1 and Q_2 are also contents obtained from experiment(s). It will be seen that relation (5) is well compatible with our experimental data for Mn–O bond length (figure 2, dashed curve c). Therefore, the *liquid drop* model looks suitable for our case.

3. Experiments

The samples used were prepared by the sol–gel method. $La(NO_3)_3$, $Sr(NO_3)_2$, $Mn(NO_3)_2$ and citric acid were mixed stoichiometrically with a nominal doping level of $La_{0.85}Sr_{0.15}MnO_3$. The resultant powder was pressed into discs 10 mm in diameter and 1.2 mm in thickness, then sintered at different temperatures, from 800 to 1400 °C, for 6 h and furnace cooled in air, to obtain a series of granular samples with different average crystal size. The patterns of x-ray diffraction showed that the lattice was in the perovskite structure and there were no impurity phases in the samples.

The average grain sizes were estimated by means of the Scherrer formula [20] by measuring the linewidths of the x-ray pattern. The formula is given by

$$D = 0.89\lambda/\sqrt{B_m^2 - B_s^2}\cos\theta$$

where D is the average diameter of the crystal grain, λ the wavelength of the x-rays, θ the angle of diffraction, B_m the measured half-peak widths of samples, and B_s the half-peak width of the bulk crystal of SiO_2 used to calibrate the intrinsic width associated with the instruments. Here the peak in the [200] orientation was measured. The peak types for samples sintered at different temperatures, normalized to the intensity, are shown in the inset of figure 1. The [200] peak just reflects the Mn–O bond length. The value D obtained from 24.4 nm to about 240 nm with the sintering temperature T_s enhanced from 800 to 1400 °C, as shown in figure 1. This result was in good agreement with that observed through the transmission electron microscope (TEM) for the samples with grain size less than 60 nm, and a little different from that observed through the scanning electron microscope (SEM) for the ones with grain size exceeding 60 nm.

The magnetization of samples was measured with a vibrating sample magnetometer (VSM) under an external field of $H = 0.12$ T.

4. Results and discussion

With grain growth, the lattice parameters were found to be enlarged, as can be seen in figure 2. Firstly, the compound is in the cubic structure ($Pm3m$, $a = b = c/\sqrt{2} = 5.498$ Å) for the 800 °C sintered sample, and the lattice undergoes a structural phase transition from a cubic perovskite to orthorhombic form ($Pbnm$) as T_s increases from 800 to 900 °C. It is worthwhile to point out that, according to our experiments, the samples synthesized from the sol–gel method an sintered at a temperature lower than 750 °C are still in an amorphous state for the La–Sr–Mn–O system. Secondly, as grain size increases, the lattice continuously deforms. Lattice parameters c and b increase. whereas a is basically invariant, and a, b, and c remain in the relation $a < c/\sqrt{2} < b$. These structural variations with the change of grain size may be attributed to the surface stress of grains as described earlier. Parameter c reflects the Mn–O bond length d_{Mn-O} ($c = 4d_{Mn-O}$). According to experimental results (the symbols in the figure), equation (5) now can be rewritten as

$$r = 7.709 + 1.225 \times 10^{-2}\ln(D) \tag{6}$$

where r and D are in ångströms. The dashed curve c in figure 2 was just calculated from (6), which, as can be seen, is very consistent with the experimental data.

The temperature dependence of magnetization of the sample group is shown in figure 3, which informs us as follows. (i) The magnetization M decreases remarkably with increasing T_s. The relative change of M is about $\delta M/M \approx -87.6\%$ as sintering temperature increases from 800 to 1400 °C. (ii) The Curie temperature T_C also decreases a little as T_s increases.

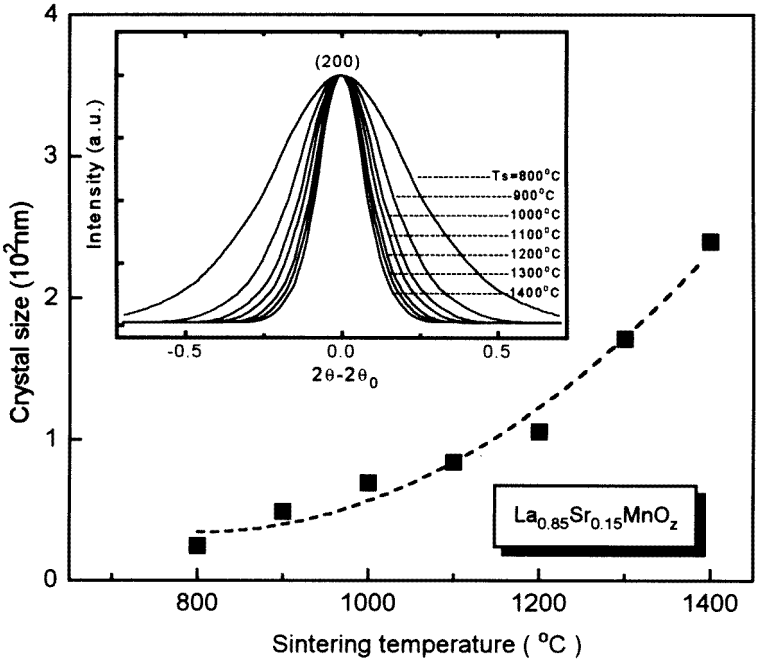

Figure 1. Grain size as a function of sintering temperature for the granular perovskite $La_{0.85}Sr_{0.15}MnO_3$. Inset, peak types in [200] orientation for samples of $La_{0.85}Sr_{0.15}MnO_3$ sintered at different temperatures, $2\theta_0 = 46.63^\circ$.

This fact has been confirmed by the experiment of differential scanning calorimetry (DSC), as shown in figure 4. (iii) Samples with smaller average grain size have M–T curves with larger slope (dM/dT). Incidentally, the 1400 °C sintered sample has nearly all the crystal features. Its transport and magnetoresistive properties are shown in the inset of figure 3.

The statements (i) and (ii) are exactly contrary to those obtained by Sánchez *et al* [15]. In their case, both magnetization and T_C increased with enlargement of grain size of $La_{0.67}Ca_{0.33}MnO_3$. We suppose that the contradiction could originate from the different concentrations of their samples and ours, since the structure or magnetism is sensitive to doping as presented in [10]. The compound with the dopant level of 0.15 we used just locates in the transition boundary from spin-canted insulator to ferromagnetic metal. This could make our samples possess some magnetic properties different from the ones with concentrations well below or above ours. Thus, it looks as if the present results make sense for other magnetic nanocrystalline materials but only for the CMR perovskite with some given compositions.

Through measuring oxygen content, with a method of iodometric titration [21], only slight oxygen surplus has been observed for our samples. The value z changed from about 3.02 to 3.01 with T_s increasing from 800 to 1400 °C. Such a small oxygen surplus could not be enough to induce such a great magnetization decrease as shown in figure 3. In the theory of double exchange, the magnetization M is given by [22, 23]

$$M \propto xb/4|J|S^2 \tag{7}$$

where b is the transfer integral between neighbouring Mn ions, S the ionic spin, J the intra-atomic exchange integral, and x the doping level of the compound. In the present case,

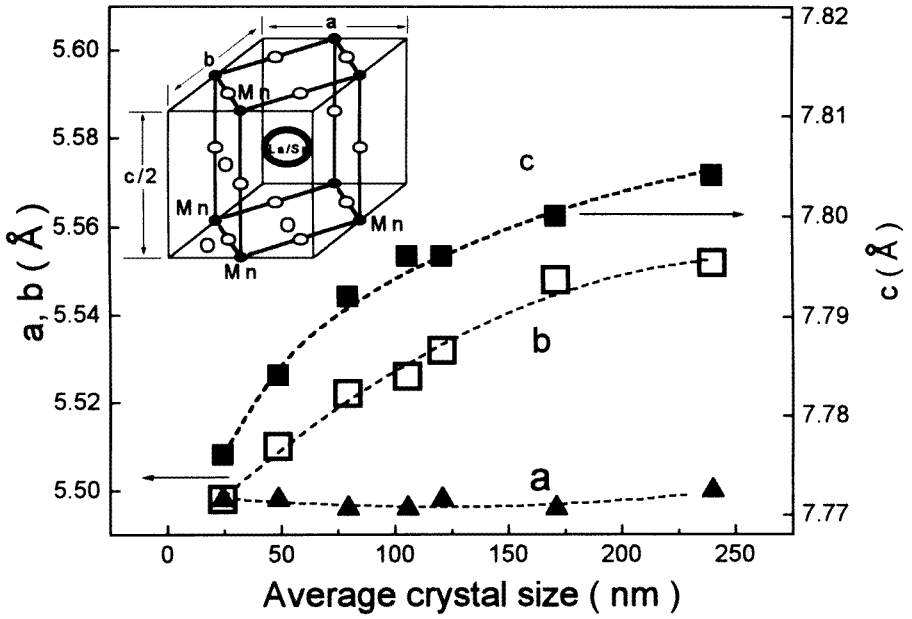

Figure 2. Lattice parameters as functions of average grain size for $La_{0.85}Sr_{0.15}MnO_3$. The dashed curve c was drawn from formula (6). Inset a schematic illustration of the perovskite structure.

there are two factors that can possibly influence M, i.e. x and b. The change of oxygen content (from 3.02 to 3.01) can lead to an average manganese oxidation state decrease from 3.19 to 3.17. This means the pairs of Mn^{3+} and Mn^{4+} decrease and could be consistent with x decreasing from 0.19 to 0.17. Consequently, we work out $\delta M/M \approx -10.53\%$ from (7). This value is much lower than the experimental data, 87.6%. Evidently, the M decrease cannot be attributed to the difference of oxygen content. Incidentally, the deviation of the calculated doping level (0.17–0.19) from the nominal value of 0.15 is advantageous for explaining the T_C difference between the results in [10] and ours. In addition, it is also impossible to attribute the present results to exchange coupling between neighbouring grains for such soft magnetic material. Hysteric measurements showed that no coercivity and remanence are observed in our samples. Therefore, it is difficult to imagine that there exists a magnetic exchange coupling between such grains which is strong enough to increase the magnetization of the system so much.

The change of lattice parameters, especially the increase of Mn–O bond length d_{Mn-O} with grain growth, needs to be taken into account. The increase of d_{Mn-O} means decreasing the overlap between the Mn^+ ion and the adjacent O^- ion. Therefore, the exchange integral b, which directly controls magnetic and transport properties, decreases. Evidently, lattice distortions could be expected to be mainly responsible for controlling magnetization. In addition, according to [9], reduction of oxygen content can also lead to enlargement of Mn–O bond length and decrease of magnetization simultaneously. These also suggest that d_{Mn-O} plays the main role in changing magnetization in such a system. The magnetization and T_C as functions of Mn–O bond length a shown in figure 5.

Experimental results [24, 25] and theoretical analysis [26] indicated that the compound $La_{1-x}Sr_xMnO_3$ is in a magnetic canted state when doping level $x \leqslant 0.17$. The angle

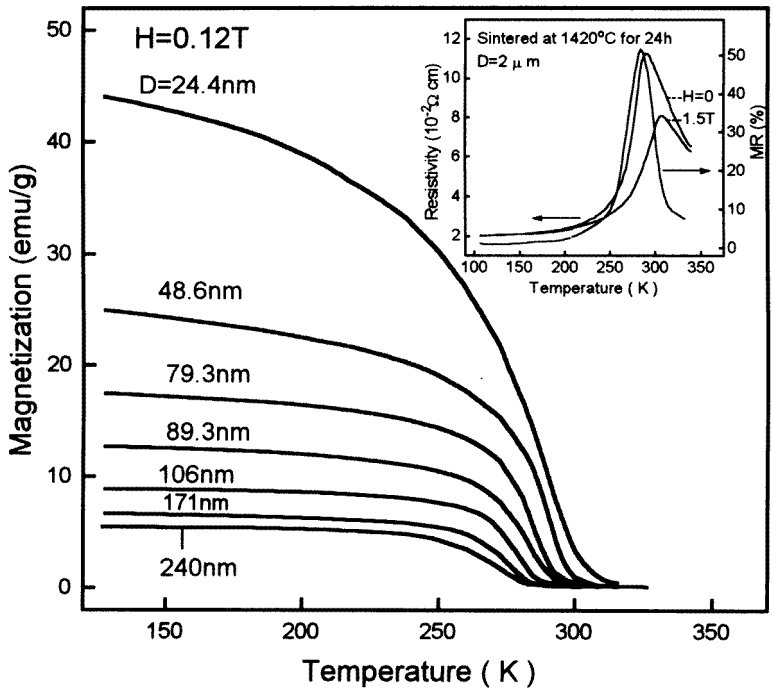

Figure 3. The magnetizations as functions of temperature for $La_{0.85}Se_{0.15}MnO_3$ samples with different grain sizes. Inset, the ρ–T curve at zero field and under an external field $H = 1.5$ T, and the corresponding MR–T curve for a 1400 °C–24 h sintered sample of $La_{0.85}Sr_{0.15}MnO_3$.

of dip of spin enlarges with increasing temperature. The magnetization increases as the angle increases near T_C, while the angle is invariant well below T_C [25]. The temperature dependent magnetization was given by the Bloch formula [27] well below T_C

$$M_s = M_0(1 - a_0T^{3/2}) \tag{8}$$

and the Dyson equation [28] near T_C

$$M_s = M_0(1 - a_0T^{3/2} - a_1T^{5/2} - a_2T^{7/2} - a_3T^4)$$

or a simplified Dyson equation

$$M_s = M_0(1 - a_0T^{3/2} - a_2T^{7/2}) \tag{9}$$

where M_s is the spontaneous magnetization, M_0 is the saturated magnetization, and a_0–a_3 are empirical constants. On the other hand, the thermal expansion of the lattice is basically linear except for a small jump near T_C [6] for the samples of $x \sim 0.2$, in other words, $d_{Mn-O} \propto T$. Therefore, we could expect the inclination angle, and so the magnetization, directly to be a function of d_{Mn-O}, at least in a narrow range of temperature. From this viewpoint, (8) and (9) can be respectively rewritten as

$$M_s = M_0(1 - a_0'd_{Mn-O}^{3/2}) \tag{10}$$

$$M_s = M_0(1 - a_0'd_{Mn-O}^{3/2} - a_2'd_{Mn-O}^{7/2}). \tag{11}$$

(10) and (11) may be called *quasi-Bloch* and *quasi-Dyson* formulas respectively. The dashed curve in figure 5 was drawn from (10). It is evidently not compatible with the

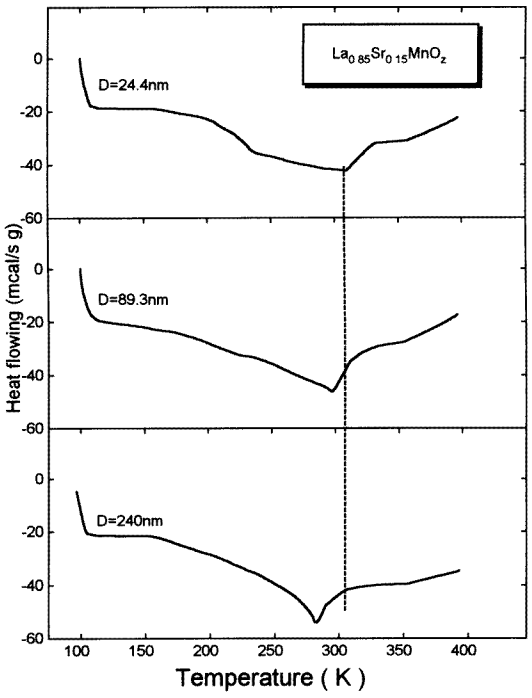

Figure 4. The DSC data for 800, 1100, and 1400 °C sintered samples of $La_{0.85}Sr_{0.15}MnO_3$.

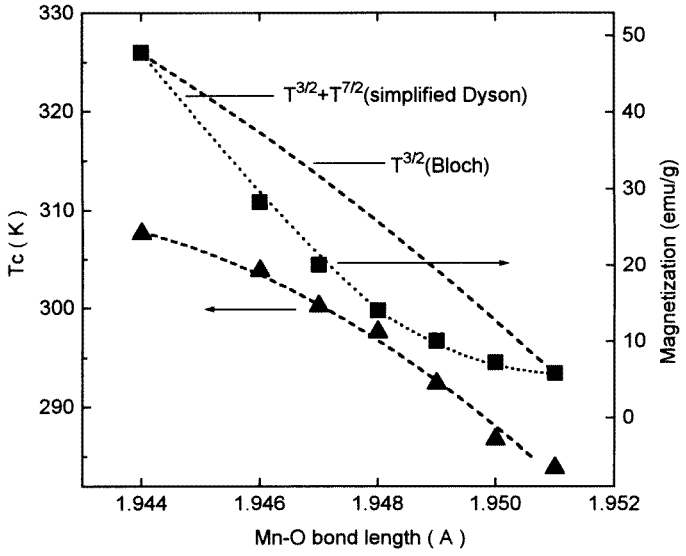

Figure 5. The magnetization and T_C under a field $H = 0.12$ T as functions of Mn–O bond length. The dashed curve was obtained by formula (10), and the dotted curve was drawn from formula (11).

experimental data. The dotted curve was obtained by using formula (11). This is in good agreement with our experiment. All these suggest that the sample with larger grain size

is in the magnetic state with a larger and easily changed angle of dip of spin. As d_{Mn-O} decreases, the exchange interaction between neighbouring Mn^{+} ions strengthens, thereby decreasing the inclination angle, that then leads to enhancing magnetization. This means a structure-coupled change of magnetism in the perovskites.

Property (iii) indicates that the ferromagnetic phase transition temperature broadens with average grain size decrease. This point can also be seen from figure 4. It suggests a wider distribution of grain size in lower-temperature sintered samples.

Additionally, there certainly exists a close interplay between the present results, i.e., the structure-coupled change of magnetism, and the CMR effect in the compound. This, at least, could lead to a shift of the onset of metal–insulator-like transition, since the CMR always takes place near T_C. However, the granular system showed a magnetoresistive behaviour very different for CMR according to [15] and our experimental results (that will be shown elsewhere). The magnetoresistance of the system appears to be a tunnelling behaviour of the grain surface and not an intrinsic crystal effect, and, for a system with the grain size small enough, such as less than 50 nm, the surface effect could be strong enough to hatch the CMR at all. This is beyond the scope of this paper. We will discuss it elsewhere.

References

[1] Chahara K-I, Ohno T, Kasai M and Kozono Y 1993 *Appl. Phys. Lett.* **63** 1990
[2] von Helmolt R, Wecker J, Holzsapfel B, Schultz L and Samwer K 1993 *Phys. Rev. Lett.* **71** 2331
[3] Jin S, Tiefel T H, McCormack M, Fastnacht R A, Ramesh R and Chen L H 1994 *Science* **264** 413
[4] Asamitsu A, Moritomo Y, Tomioka Y, Arima T and Tokura Y 1995 *Nature* **373** 407
[5] Kuwahara H, Tomioka Y, Moritomo Y, Asamitsu A, Kasai M, Kumai R and Tokura Y 1996 *Science* **272** 80
[6] Radaelli P G, Cox D E, Marezio M, Cheong S-W, Schiffer P E and Ramirez A P 1995 *Phys. Rev. Lett.* **75** 4488
[7] Moritomo Y, Asamitsu A and Tokura Y 1995 *Phys. Rev.* B **51** 16 491
[8] Hwang H Y, Cheong S-W, Radaelli P G, Marezio M and Batlogg B 1995 *Phys. Rev. Lett.* **75** 914
[9] Ju H L, Gopalakrishnan J, Peng J L, Qi Li, Xiong G C, Venkatesan T and Greene R L 1994 *Phys. Rev.* B **51** 6143
[10] Urushibara A, Moritomo Y, Arima T, Asamitsu A, Kido G and Tokura Y 1995 *Phys. Rev.* B **51** 14 103
[11] Fontcuberta J, Martinez B, Seffar A, Piñol S, García-Muñoz J L and Obradors X 1996 *Phys. Rev. Lett.* **76** 1122
[12] Argyriou D N, Mitchell J F, Potter C D, Hinks D G, Jorgensen J D and Bader S D 1996 *Phys. Rev. Lett.* **76** 3826
[13] Itoh M, Shimura T, Yu Jian-Ding, Hayashi T and Inaguma Y 1995 *Phys. Rev.* B **52** 12 522
[14] Solovyev I, Hamada N and Terakura K 1996 *Phys. Rev. Lett.* **76** 4825
[15] Sánchez R D, Rivas J, Vázquez-Vázquez C, López-Quintela A, Causa M T, Tovar M and Oseroff S 1996 *Appl. Phys. Lett.* **68** 134
[16] Zhu X, Birringer R, Herr U and Gleiter H 1987 *Phys. Rev.* B **35** 9085
[17] Lupo J A and Sabochick M J 1992 *Nanostruct. Mater.* **1** 131
[18] Guttman L 1961 *J. Chem. Phys.* **34** 1024
[19] Madelung E 1918 *Z. Phys.* **19** 524
[20] Mendelson M I, 1969 *J. Am. Ceram. Soc.* **52** 443
[21] Vanderah A T 1991 *Chemistry of Superconductor Materials* (NJ: Noyes)
[22] Anderson P W and Hasegawa H 1955 *Phys. Rev.* **100** 675
[23] deGennes P G 1960 *Phys. Rev.* **118** 141
[24] Kawano H, Kajimoto R, Kubota M and Yoshizawa H 1996 *Phys. Rev.* B **53** 2202
[25] Argyriou D N, Mitchell J F, Potter C D, Hinks D G, Jorgensen J D and Bader S D 1996 *Phys. Rev. Lett.* **76** 3826
[26] Inoue J and Maekawa S 1996 *Phys. Rev. Lett.* **76** 3826
[27] Bloch F 1931 *Z. Phys.* **61** 206
[28] Dyson F T 1956 *Phys. Rev.* **102** 1217